



Cite this: DOI: 10.1039/c8nj05668d

Received 8th November 2018,  
Accepted 10th December 2018

DOI: 10.1039/c8nj05668d

rsc.li/njc

# Synthesis and evaluation of chiral $\beta$ -amino acid-based low-molecular-weight organogelators possessing a methyl/trifluoromethyl side chain†

Koichi Kodama, \* Ryuta Kawamata and Takuji Hirose

The synthesis and gelation properties of chiral  $\beta$ -amino acid-based low-molecular-weight organogelators, possessing methyl/trifluoromethyl side chains, are reported. The structure of the side chain and chirality were found to be important parameters affecting the gelation ability. The pure enantiomer of the trifluoromethylated  $\beta$ -amino acid displayed good gelation properties due to the formation of fibrillar networks, driven by enhanced amide hydrogen bonding. An investigation of the effects of the alkyl chain length showed that longer alkyl chain improved the gelation ability, yet the same supramolecular structure was observed in all, as well as an odd–even effect in both the melting points and  $T_g$  values.

## Introduction

Gels are important soft materials that have found application in a wide range of areas, from the cosmetics industry to drug delivery systems, amongst others.<sup>1</sup> Recently, low-molecular-weight gelators (LMWGs) have attracted much attention because these can be carefully designed to impart specific properties to a gel. The resultant supramolecular gels are stimuli-responsive and have been successfully employed in catalysis, biomaterials, pollutant removal, *etc.*<sup>2</sup> The mechanism of gelation is based on the entrapment of solvent molecules within entangled fibers that are made of LMWGs. Therefore, the gelation ability of LMWGs is dependent on their intermolecular interaction, resulting in self-assembly into fibrous structures.<sup>3</sup> Although various LMWGs have been developed, the design of effective LMWGs remains challenging. The ability to predict gel properties is crucial, in terms of the practical application as well as for more detailed understanding of the supramolecular chemistry. Thus, better understanding of the relationship between the chemical structure of LMWGs and their gelation ability is required.

Most LMWGs that have been developed for organic solvents, are composed of a hydrogen bonding moiety that drives self-assembly, and long alkyl chains for effective fixation of solvent molecules *via* van der Waals interactions.<sup>4</sup> Amino acids are a suitable class of compounds for the preparation of such

LMWGs, because they possess multiple hydrogen bonding groups and can be easily modified with long alkyl chains.<sup>5</sup> Furthermore,  $\alpha$ -amino acids are readily available, and thus, fatty acid amides of natural  $\alpha$ -amino acids have been thoroughly investigated in this respect, and found to display good gelation abilities for organic solvents such as toluene and hexane.<sup>6</sup> The effect of the hydrogen bonding moiety in such LMWGs has been documented. For example, replacement of the amide moiety with a stronger hydrogen bonding group, such as a urea moiety, results in higher gelation ability due to the stronger intermolecular interaction between the LMWGs, which enhances their self-assembly.<sup>7</sup>

In addition to hydrogen bonding and the alkyl chain length, the gelation ability is influenced by other more subtle structural differences in the LMWGs, such as chirality.<sup>8</sup> In most cases, a racemate displays poorer gelation ability than the pure enantiomer, *e.g.* optically pure *N*-acyl-L- $\alpha$ -alanine affords gels in toluene or hexane while the corresponding racemates do not.<sup>9</sup> However, the effect of chirality is still unclear because some racemates exhibit higher gelation ability than the corresponding pure enantiomers.<sup>10</sup> Although amides of  $\alpha$ -amino acids have been extensively studied as gelators, limited examples of the use of amides of  $\beta$ -amino acids are available. Nevertheless, it has been reported that achiral *N*-acyl- $\beta$ -alanine without a side chain exhibits poorer gelation ability than the branched *N*-acyl-L- $\alpha$ -alanine with the same molecular formula.<sup>11</sup> Thus, it can be deduced that both chirality and the presence of a side chain in *N*-acyl-L- $\alpha$ -alanine play an important role in gel formation. This prompted us to investigate branched chiral  $\beta$ -amino acids as candidates for potential LMWGs for organic solvents. Chiral supramolecular gels are attractive materials because they have been applied to asymmetric synthesis, enantiomer separation and so on.<sup>12</sup>

Department of Applied Chemistry, Graduate School of Science and Engineering, Saitama University, 255 Shimo-Okubo, Sakura-ku, Saitama, 338-8570, Japan.

E-mail: kodama@mail.saitama-u.ac.jp

† Electronic supplementary information (ESI) available: Detailed experimental procedure, XRD patterns of (*S*)-**1m**, summary of crystallographic data, copies of <sup>1</sup>H, <sup>13</sup>C, <sup>19</sup>F NMR and IR spectra. CCDC 1865320–1865322. For ESI and crystallographic data in CIF or other electronic format see DOI: 10.1039/c8nj05668d

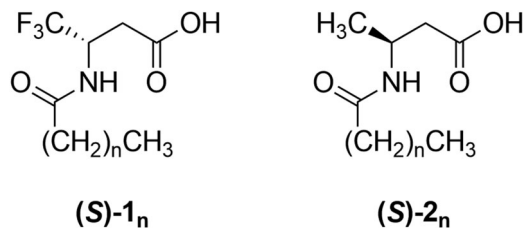


Fig. 1 Structures of amide derivatives of chiral  $\beta$ -amino acids ( $S$ )- $1_n$  and ( $S$ )- $2_n$ .

Herein, we describe amide derivatives of a chiral  $\beta$ -amino acid  $1_n$  possessing a trifluoromethyl group as potential LMWGs and the corresponding methyl analogues  $2_n$  derived from  $\beta$ -homocysteine (Fig. 1). It was envisaged that the side chains of  $1_n$  and  $2_n$  would improve the gelation ability, and furthermore, that the electron-withdrawing trifluoromethyl group of  $1_n$  would enhance the hydrogen bond of the neighboring amide moiety, thereby assisting in the formation of fibrous aggregates. This effect of the trifluoromethyl moiety was observed in a study in which ( $S$ )- $1$  units were incorporated within a peptide hexamer. The hexamer adopted a stable helically folded structure due to stronger intramolecular hydrogen bonds between the amide moieties, attributed to the trifluoromethyl moiety.<sup>13</sup> Therefore, in this present study, optically pure and racemic  $1_n$  and  $2_n$  were synthesized to investigate the effects of the following variables on the gelation behavior: (1) branched side chains on the  $\beta$ -amino acid, (2) chirality, and (3) fluorinated side chains.

## Results and discussion

### Synthesis and gelation behavior of $1_6$ and $2_6$

The racemic and enantiopure forms of  $1_n$  and  $2_n$  were synthesized by an amide coupling reaction between esters of the corresponding  $\beta$ -amino acids and linear aliphatic carboxylic acids, followed by hydrolysis of the ester (see ESI,† Schemes S1–S4). The precursor esters of the  $\beta$ -amino acids were synthesized according to the literature procedures.<sup>14</sup> Initially, amide derivatives  $1_6$  and  $2_6$ , prepared from octanoic acid ( $n = 6$ ), were investigated. The melting points and gelation properties of ( $S$ )/ $rac$ - $1_6$  and ( $S$ )/ $rac$ - $2_6$  with three organic solvents (toluene, chloroform, and tetrachloromethane) are summarized in Table 1, accompanied by the data of linear achiral  $N$ -octanoyl- $\beta$ -alanine ( $C_6$ - $\beta$ -Ala) for comparison.

Enantiopure ( $S$ )- $2_6$  with a branched methyl group did not afford a gel with any of the tested solvents. This was similarly observed for  $C_6$ - $\beta$ -Ala.  $rac$ - $2_6$  displayed slight gelation ability with toluene and tetrachloromethane. The melting points of  $2_6$  were about 20 °C lower than that of  $C_6$ - $\beta$ -Ala, indicating weaker intermolecular interactions between  $2_6$  molecules. This was attributed to the methyl side chain of  $2_6$ , which prevents dense molecular packing.

In contrast to ( $S$ )- $2_6$ , ( $S$ )- $1_6$  possessing a trifluoromethyl group displayed high gelation ability with all the three solvents. In particular, a transparent organogel was obtained with the

Table 1 Melting points of ( $S$ )/ $rac$ - $1_6$ , ( $S$ )/ $rac$ - $2_6$ , and  $C_6$ - $\beta$ -Ala and their gelation ability in different solvents<sup>a</sup>

Compound	Mp (°C)	PhCH <sub>3</sub>	CHCl <sub>3</sub>	CCl <sub>4</sub>
( $S$ )- $1_6$	121–123	G (3.4)	G (18.7)	G (8.9)
$rac$ - $1_6$	138–139	I	G (50.0)	I
( $S$ )- $2_6$	83–84	P	S	I
$rac$ - $2_6$	78–80	G (54.2)	S	G (130)
$C_6$ - $\beta$ -Ala	99–101	P	S	I

<sup>a</sup> The values in parentheses represent minimum gelation concentration (MGC, g L<sup>-1</sup>). G = gelation, I = insoluble, P = precipitate, S = soluble.

lowest MGC value (3.4 g L<sup>-1</sup>) for toluene. The melting point of ( $S$ )- $1_6$  was higher than those of ( $S$ )- $2_6$  and  $C_6$ - $\beta$ -Ala, which indicates that the self-assembly of ( $S$ )- $1_6$  to form a supramolecular structure is enhanced, despite the steric effect of the trifluoromethyl side chain. The gelation ability of  $rac$ - $1_6$  was less than that of ( $S$ )- $1_6$  because of its lower solubility (consistent with its higher melting point). A similar trend due to chirality was observed for  $N$ -acyl- $\alpha$ -alanine.<sup>9</sup> The difference in properties between  $1_6$  and  $2_6$  were primarily attributed to the stronger hydrogen bonds of the amide moiety in  $1_6$  than in  $2_6$ .

The organogel of ( $S$ )- $1_6$  in toluene was stable at room temperature and collapsed to give a clear solution upon heating. The gel/solution transitions were reversible by the repeated heating-cooling process. The thermal stability of the gel was evaluated based on the gel-to-sol transition temperatures ( $T_g$ ) at various concentrations of ( $S$ )- $1_6$  (Fig. 2). The  $T_g$  value at the MGC was 49 °C and it gradually increased to 80 °C with increasing concentration of ( $S$ )- $1_6$ . This indicates that the growth of fibrillar aggregates by intermolecular interactions was enhanced at higher concentrations. The  $T_g$  value is higher than that of previously reported  $N$ -octadecanoyl- $L$ - $\alpha$ -alanine in toluene with a similar concentration, despite the significantly shorter alkyl chain of ( $S$ )- $1_6$ .<sup>9</sup>

### SEM, XRD, and IR spectra of xerogels

The microstructure of the LMWGs in the organogels was characterized by drying the gels in air, followed by analysis of the powdery LMWG solids (xerogels) by FE-SEM, FT-IR, and

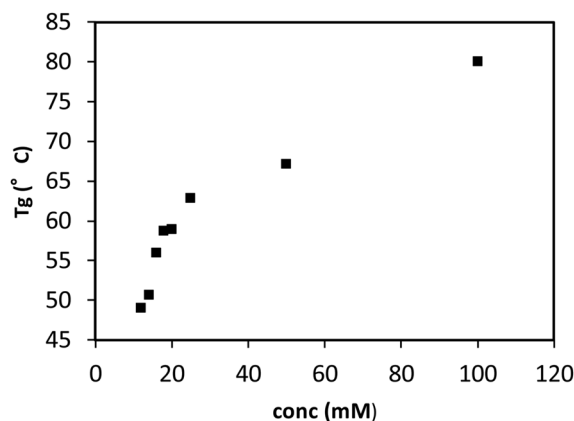


Fig. 2 Plot of gel-to-sol transition temperatures ( $T_g$ ) with different concentrations of ( $S$ )- $1_6$  in toluene.

XRD measurements. The SEM images of the solids (Fig. 3) revealed that fibrous aggregates were constructed and three-dimensionally entangled in (*S*)-**1<sub>6</sub>** and *rac*-**2<sub>6</sub>**. The densely entangled thin fibers of (*S*)-**1<sub>6</sub>** (0.25–1.0 μm in diameter) indicate stable gel formation in toluene or chloroform. Thicker bundled fibers (2–3 μm in diameter) were observed for *rac*-**2<sub>6</sub>**, which is indicative of less efficient 1D growth of the aggregates. In contrast, a short, thick, tape-like morphology was observed for the xerogel of *rac*-**1<sub>6</sub>** prepared from its chloroform gel, indicative of its crystalline character rather than good gelation property.

In the IR spectrum of (*S*)-**1<sub>6</sub>** in the solid state, characteristic absorption bands were observed at 3297 and 1666 cm<sup>-1</sup>, corresponding to the hydrogen-bonded N–H and C=O stretching vibrations of the amide group. Similar absorption bands were observed at 3354 and 1627 cm<sup>-1</sup> for *rac*-**1<sub>6</sub>**, at 3316 and 1645 cm<sup>-1</sup> for (*S*)-**2<sub>6</sub>**, and at 3296 and 1645 cm<sup>-1</sup> for *rac*-**2<sub>6</sub>**. Given the similarity in the positions of the absorption bands of the amide moiety in solid C<sub>6</sub>-β-Ala (3357 and 1684 cm<sup>-1</sup>),<sup>6b</sup> it was deduced that hydrogen bonds were formed by the amide group of LMWGs **1<sub>6</sub>** and **2<sub>6</sub>**.

The XRD patterns of all the compounds showed one intense reflection peak (Fig. 4). Despite the likeness in molecular shape and size, the *d*-spacing values were completely different. The molecular length of the extended structure was calculated to be 1.5 nm, which was taken as the distance between the carboxy oxygen atom and the terminal of the alkyl chain. The *d*-spacing values of (*S*)-**2<sub>6</sub>**, *rac*-**2<sub>6</sub>**, and C<sub>6</sub>-β-Ala were much larger than the estimated molecular length, which is indicative of bilayer structures, constructed by hydrogen bonded carboxylic acid dimers. Such a bilayer structure is a generally proposed model for LMWGs of amide derivatives of amino acids. The shorter *d*-spacing of (*S*)-**2<sub>6</sub>** and *rac*-**2<sub>6</sub>** of twice the molecular length was attributed to the interdigitation of alkyl chains or tilting of the dimers relative to the plane of the bilayer. The slightly shorter *d*-spacing of *rac*-**2<sub>6</sub>** than that of (*S*)-**2<sub>6</sub>** might indicate that the dimers are stacked by stronger hydrogen bonds, causing them to tilt relative to the plane of the layer. It is noteworthy that the

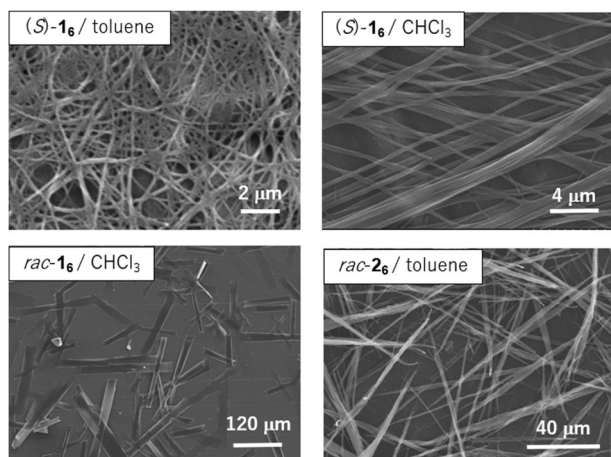


Fig. 3 SEM images of the xerogels of **1<sub>6</sub>** and **2<sub>6</sub>**.

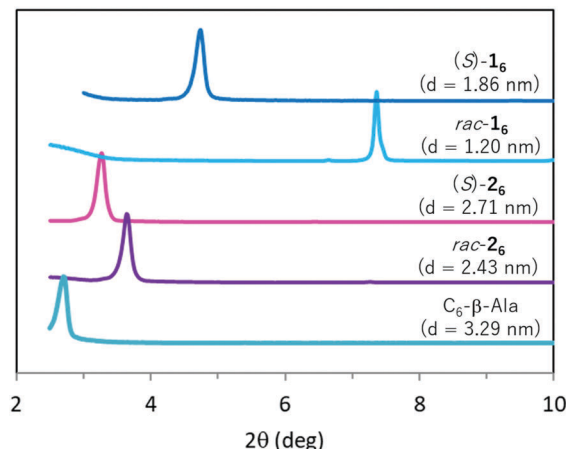


Fig. 4 XRD patterns of the xerogels **1<sub>6</sub>**, **2<sub>6</sub>**, and C<sub>6</sub>-β-Ala.

*d*-spacing value of (*S*)-**1<sub>6</sub>** was significantly shorter than that of (*S*)/*rac*-**2<sub>6</sub>**. Furthermore, the *d*-spacing of *rac*-**1<sub>6</sub>** was 1.20 nm, which was shorter than the estimated molecular length. It was suggested that the electron-withdrawing trifluoromethyl group enhanced the hydrogen bonding ability of the amide moiety of **1<sub>6</sub>**, thereby leading to the loss of the carboxylic acid dimer structure and a change in the molecular packing.

#### X-ray crystallographic analysis of C<sub>6</sub>-β-Ala and *rac*-**1<sub>6</sub>**

It was proposed that C<sub>12</sub>-β-Ala served as a LMWG as fibrous supramolecular structures were constructed due to carboxylic acid dimer formation and intermolecular hydrogen bonds between the amide moieties.<sup>15</sup> To obtain more insight into the supramolecular structure of the LMWGs in this study, X-ray crystallographic analysis of C<sub>6</sub>-β-Ala was conducted. Slow evaporation of the ethanol solution of C<sub>6</sub>-β-Ala afforded two polymorphic crystals: needle-like crystals and thin plate-like crystals. Analysis of the structure of the needle-like crystal indicated that the molecules adopted an all-*trans* conformation and hydrogen-bonded carboxylic acid dimers were formed (Fig. 5a). As expected, the dimers were combined with hydrogen bonds between the amide moieties to afford a 1D hydrogen bonding network. The 1D networks were arranged to form a bilayer structure (Fig. 5b). The molecules are tilted with respect to the layer and the interlayer distance was 2.65 nm, which is shorter than the *d*-spacing value of C<sub>6</sub>-β-Ala, as estimated from the XRD pattern of its powdered solid (3.29 nm, Fig. 4). The structure of the plate-like crystal (Fig. 5c) was similar to that of the needle-like crystal except that the dimers are combined two-dimensionally by amide hydrogen bonds to form a bilayer structure. Such a difference resulted from the *gauche* conformation of the octanoyl and hydroxycarbonylmethyl moieties. The distance between the two bilayers was 3.09 nm, which is close to the *d*-spacing value of the powdered solid. The slightly shorter distance was attributed to the lower measurement temperature. It is speculated that the comparable *d*-spacing values of (*S*)/*rac*-**2<sub>6</sub>** and C<sub>6</sub>-β-Ala are due to the formation of similar supramolecular structures. It is noteworthy that C<sub>6</sub>-β-Ala afforded a concomitant polymorph because its flexible

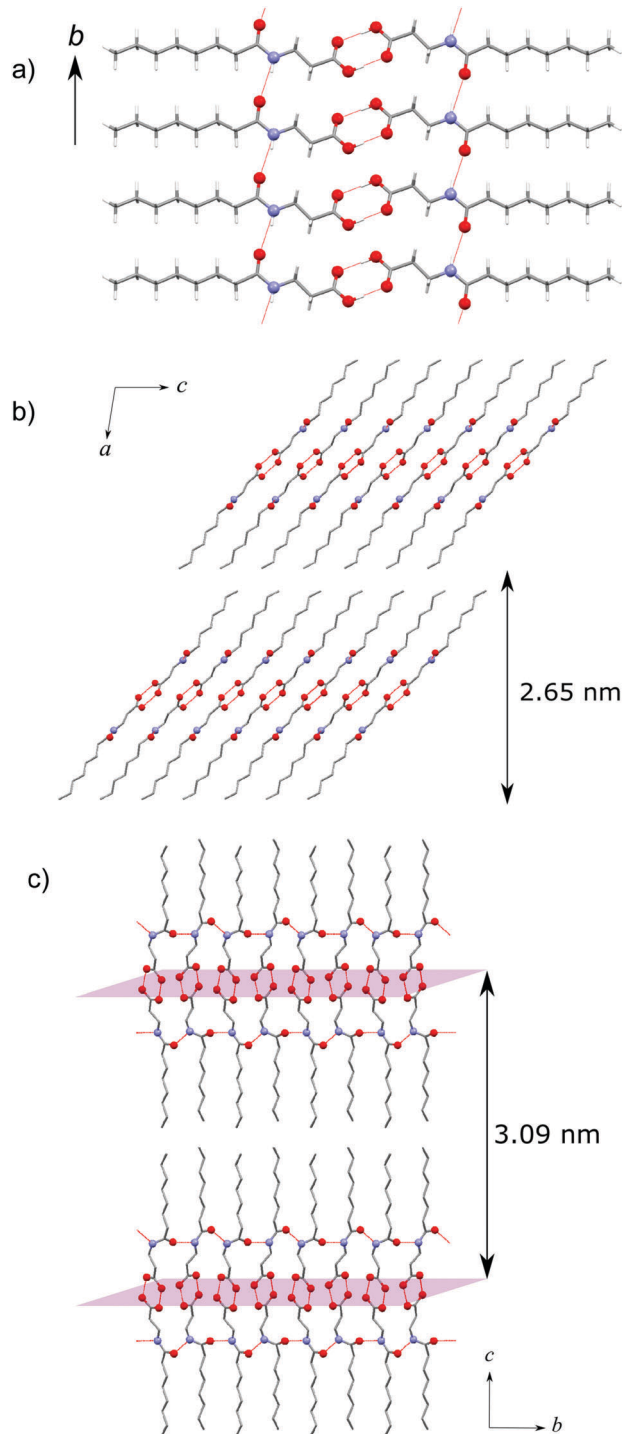


Fig. 5 Crystal structures of  $C_6$ - $\beta$ -Ala. (a) One dimensional hydrogen-bonding network, (b) bilayer structures of needle-like crystal and (c) hydrogen-bonded two dimensional bilayers of plate-like crystal.

ethylene backbone afforded two stable conformational isomers. On the other hand, the presence of the side chain on the  $\beta$ -amino acids in  $1_n$  and  $2_n$  can restrict the molecular conformation to favor one morphology over another.

Fortunately, slow diffusion of hexane into the ethyl acetate solution of *rac*- $1_6$  afforded needle-like crystals suitable for

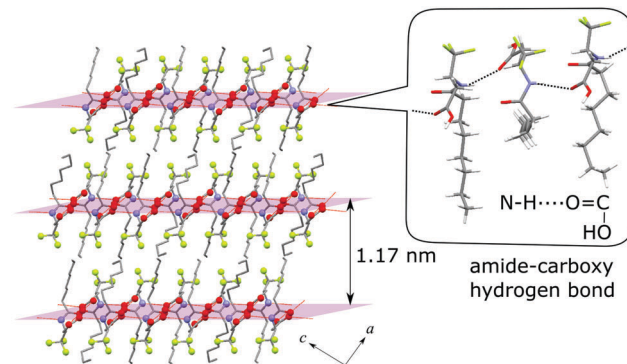


Fig. 6 Crystal structure of *rac*- $1_6$ .

crystallographic analysis. The structure is shown in Fig. 6. Both enantiomers of  $1_6$  were included in a ratio of 1:1 to form a racemic compound. In contrast to  $C_6$ - $\beta$ -Ala, the carboxylic acid dimers were not formed. Instead, the carboxy oxygen was hydrogen bonded to the amide hydrogen of the neighboring molecule. Since hydrogen bonds are often formed between the best hydrogen-bond donor and the best hydrogen-bond acceptor, the amide hydrogen, which was enhanced by the trifluoromethyl group, formed a hydrogen bond with a stronger acceptor.<sup>16</sup> The enantiomers alternated to avoid steric repulsion between the trifluoromethyl groups. The 1D self-assembled structures were further connected by hydrogen bonds between the carboxy hydrogen and amide oxygen to form a 2D layer structure. The interlayer distance corresponding to the diffraction from the (101) face was 1.17 nm, which is close to the *d*-spacing value (1.20 nm) obtained from the XRD measurement. The octanoyl group was not only partly folded, but also tilted relative to the layer, which resulted in a much shorter *d*-spacing value than the calculated molecular length of  $1_6$ . Such a 2D hydrogen bonding network is consistent with the tape-like morphology of *rac*- $1_6$  by SEM observation (Fig. 3) and should result in a higher melting point and lower solubility than (*S*)- $1_6$ .

Although the detailed supramolecular structure of enantiopure (*S*)- $1_6$  has not yet been revealed, the XRD data and SEM observation indicate that (*S*)- $1_6$  constructs 1D networks due to the hydrogen bonds between its amide and carboxy groups (Fig. 7a), most likely due to efficient molecular packing during homochiral aggregation. The stronger hydrogen bonds and preferential formation of a 1D network compared to (*S*)- $2_6$  (Fig. 7b) should result in the higher gelation property.

#### Effect of alkyl chain length of (*S*)- $1_n$

To investigate the effect of alkyl chain length and develop better LMWGs, (*S*)- $1_n$  with longer alkyl chains ( $n = 7-10$ ) were investigated. Their melting points and gelation ability in toluene are summarized in Table 2. With increasing alkyl chain length, the MGC values for toluene gradually decreased and only  $2.6 \text{ g L}^{-1}$  of (*S*)- $1_{10}$  afforded a gel in toluene, which is due to the stronger van der Waals interaction between the alkyl chains. All the XRD patterns of the LMWGs (*S*)- $1_n$  showed one intense diffraction peak (Fig. S1, ESI<sup>†</sup>). The *d*-spacing values increased with increasing alkyl chain number. This result indicates that a common supramolecular

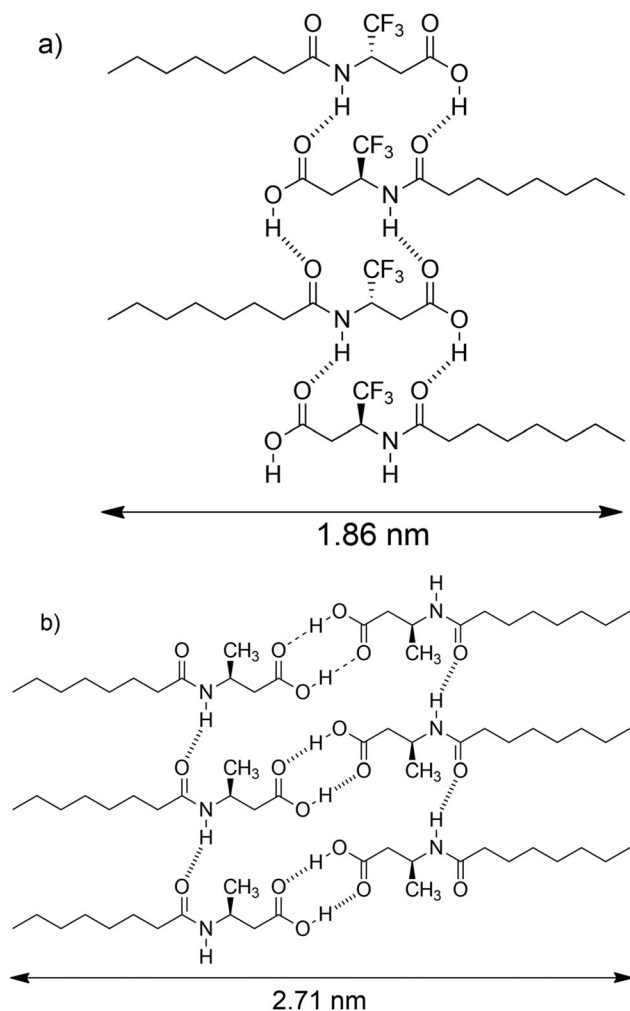


Fig. 7 Proposed supramolecular structure of (a) (*S*)-**1**<sub>6</sub> and (b) (*S*)-**2**<sub>6</sub>.

Table 2 Melting points, gelation ability in toluene and XRD data of (*S*)-**1**<sub>*n*</sub>

Compound	Mp (°C)	MGC (g L <sup>-1</sup> )	<i>T</i> <sub>g</sub> <sup>a</sup> (°C)	<i>d</i> -Spacing (nm)
( <i>S</i> )- <b>1</b> <sub>6</sub>	121–123	3.4	80	1.86
( <i>S</i> )- <b>1</b> <sub>7</sub>	125–128	3.6	85	1.98
( <i>S</i> )- <b>1</b> <sub>8</sub>	125–128	3.1	82	2.11
( <i>S</i> )- <b>1</b> <sub>9</sub>	127–130	3.1	88	2.18
( <i>S</i> )- <b>1</b> <sub>10</sub>	127–129	2.6	85	2.37

<sup>a</sup> *T*<sub>g</sub> values were measured for the 0.1 M samples in toluene.

structure is adopted by all (*S*)-**1**<sub>*n*</sub>. Interestingly, an odd–even effect of the alkyl chain numbers in the melting points and *T*<sub>g</sub> values was observed. The melting points of (*S*)-**1**<sub>*n*</sub> gradually increased every two chain numbers and the *T*<sub>g</sub> values with odd-numbered alkyl chains were slightly higher than the even-numbered ones, which has some implication on the packing of neighboring alkyl chains during the aggregation of (*S*)-**1**<sub>*n*</sub>.<sup>17</sup>

## Conclusions

Racemic and enantiopure LMWGs derived from chiral β-amino acids, and possessing a methyl or trifluoromethyl side chain,

were synthesized and their gelation ability in organic solvents was examined. Branching due to the methyl group of β-amino acids **2**<sub>6</sub> prevented molecular packing, decreasing the intermolecular interactions. The pure enantiomer of the trifluoromethylated β-amino acid derivative (*S*)-**1**<sub>6</sub> showed higher gelation ability in organic solvents than other LMWGs. From the characterization of these LMWGs, it was clear that the trifluoromethyl group of **1**<sub>6</sub> enhanced the hydrogen bonding capability of the neighboring amide group, and hydrogen bonds between the amide and carboxy moieties afforded a different supramolecular structure to the methyl-substituted **2**<sub>6</sub>. While *rac*-**1**<sub>6</sub> afforded a layered network to avoid steric hindrance between the trifluoromethyl side chains, 1D fibrous structures were constructed in enantiopure (*S*)-**1**<sub>6</sub>. The gelation ability was further improved in (*S*)-**1**<sub>*n*</sub> with increasing alkyl chain length. All (*S*)-**1**<sub>*n*</sub> compounds adopted a similar molecular assembly with an odd–even effect of the alkyl chain on the gelation ability. The insight obtained in this study will make a significant contribution to the design of more effective LMWGs for use in various applications.

## Experimental section

### Characterization methods

The <sup>1</sup>H, <sup>13</sup>C, and <sup>19</sup>F NMR spectra were recorded on 300, 400, or 500 MHz Bruker Avance II spectrometers. Chemical shifts of <sup>1</sup>H and <sup>13</sup>C NMR are quoted relative to tetramethylsilane (δ = 0.0 ppm) as an internal standard, and those of <sup>19</sup>F NMR are quoted relative to trifluorotoluene (δ = –63.7 ppm) as an external standard. IR spectra were measured at room temperature using a JASCO FT-IR 460, and absorption maxima (*ν*<sub>max</sub>) are quoted in wavenumbers (cm<sup>-1</sup>). Melting points were measured using a Mitamura Riken Kogyo MEL-TEMP and are reported uncorrected. High-resolution MALDI-TOF mass spectra were recorded using a Bruker Autoflex III mass spectrometer. Powder X-ray diffraction (XRD) patterns were measured using a Bruker D2 PHASER diffractometer with CuKα radiation at room temperature. Scanning electron microscopy (SEM) measurements of the dried samples that were placed on aluminum foil were obtained at 15 kV using a HITACHI S-2400. X-ray crystallographic data were collected with graphite monochromated MoKα radiation using a Bruker SMART APEX II diffractometer. Data collections were carried out at 100 or 150 K. The structures were solved by a direct method and refined by SHELXL-2013 or SHELXL-2018/1 programs.<sup>18</sup> Crystallographic information files have been deposited in the Cambridge Structural Database (CCDC 1865320–1865322).<sup>†</sup>

### Synthesis

The compounds (*S*)/*rac*-**1**<sub>*n*</sub> and (*S*)/*rac*-**2**<sub>6</sub> were synthesized from the corresponding esters of the β-amino acids, which were prepared according to literature procedures.<sup>13</sup> The detailed syntheses and characterization data have been provided in the ESI.<sup>†</sup>

## Determination of gelation properties

A solid sample (5 mg) was placed in a test tube and the solvent was added whilst heating on a hot plate. Insoluble solid was denoted as “I” (insoluble). If the solid dissolved, the solution was allowed to stand at room temperature. The precipitate that formed was denoted as “P” (precipitate). Gelation was confirmed by flow in the tube inversion test method. If a drop was observed, it was denoted as “S” (soluble). If not, it was denoted as “G” (gel). Upon formation of a gel, the procedure was repeated with addition of the solvent until no gelation was observed. Thus, the lowest concentration of the sample that was required to afford a gel was determined, and this was defined as the minimum gelation concentration (MGC, g L<sup>-1</sup>). The thermal stability of the gels was evaluated by the gel-to-sol transition temperature ( $T_g$ ), which was defined as the temperature at which the gel started to collapse due to heating.

## Conflicts of interest

There are no conflicts to declare.

## Acknowledgements

We thank to Dr Yasuhiro Ishida (RIKEN) for giving the samples for the synthesis of (S)-1.

## Notes and references

- 1 J. Meyr, C. Saldias and D. D. Diaz, *Chem. Soc. Rev.*, 2018, **47**, 1484–1515.
- 2 (a) F. R. Llansola, B. Escuder and J. F. Miravet, *J. Am. Chem. Soc.*, 2009, **131**, 11478–11484; (b) X. Yu, L. Chen, M. Zhang and T. Yi, *Chem. Soc. Rev.*, 2014, **43**, 5346–5371; (c) K. J. Skilling, F. Citossi, T. D. Bradshaw, M. Ashford, B. Kellam and M. Marlow, *Soft Matter*, 2014, **10**, 237–256; (d) X. Du, J. Zhou, J. Shi and B. Xu, *Chem. Rev.*, 2015, **115**, 13165–13307; (e) B. O. Okesola and D. K. Smith, *Chem. Soc. Rev.*, 2016, **45**, 4226–4251.
- 3 (a) A. R. Hirst, I. A. Coates, T. R. Boucheteau, J. F. Miravet, B. Escuder, V. Castelletto, I. W. Hamley and D. K. Smith, *J. Am. Chem. Soc.*, 2008, **130**, 9113–9121; (b) L. E. Buerkle and S. J. Rowan, *Chem. Soc. Rev.*, 2012, **41**, 6089–6102.
- 4 J. H. van Esch, *Langmuir*, 2009, **25**, 8392–8394.
- 5 (a) M. Suzuki and K. Hanabusa, *Chem. Soc. Rev.*, 2009, **38**, 967–975; (b) C. Tomasini and N. Castellucci, *Chem. Soc. Rev.*, 2013, **42**, 156–172; (c) K. Hanabusa and M. Suzuki, *Bull. Chem. Soc. Jpn.*, 2016, **89**, 174–182.
- 6 (a) N. Zweep, A. Hopkinson, A. Meetsma, W. R. Browne, B. L. Feringa and J. H. van Esch, *Langmuir*, 2009, **25**, 8802–8809; (b) A. Pal, R. D. Mahapatra and J. Dey, *Langmuir*, 2014, **30**, 13791–13798.
- 7 (a) F. Fages, F. Vögtle and M. Žinić, *Top. Curr. Chem.*, 2005, **256**, 77–131; (b) A. Pal and J. Dey, *Langmuir*, 2011, **27**, 3401–3408.
- 8 (a) K. Hanabusa, M. Yamada, M. Kimura and H. Shirai, *Angew. Chem., Int. Ed.*, 1996, **35**, 1949–1951; (b) V. Čaplar, M. Žinić, J. L. Pozzo, F. Fages, G. Mieden-Gundert and F. Vögtle, *Eur. J. Org. Chem.*, 2004, 4048–4059; (c) A. Brizard, R. Oda and I. Huc, *Top. Curr. Chem.*, 2005, **256**, 167–218; (d) V. Čaplar, L. Frkanec, N. Š. Vujičić and M. Žinić, *Chem. – Eur. J.*, 2010, **16**, 3066–3082; (e) A. Pal and J. Dey, *RSC Adv.*, 2014, **4**, 17521–17525.
- 9 A. Pal, Y. K. Ghosh and S. Bhattacharya, *Tetrahedron*, 2007, **63**, 7334–7348.
- 10 (a) A. R. Borges, M. Hyacinth, M. Lum, C. M. Dingle, P. L. Hamilton, M. Chruszcz, L. Pu, M. Sabat and K. L. Caran, *Langmuir*, 2008, **24**, 7421–7431; (b) K. Kohno, K. Morimoto, N. Manabe, T. Yajima, A. Yamagishi and H. Sato, *Chem. Commun.*, 2012, **48**, 3860–3862.
- 11 A. Pal, T. Patra and J. Dey, *Chem. Phys. Lett.*, 2013, **556**, 245–250.
- 12 (a) A. Dawn, N. Fujita, S. Haraguchi, K. Sada and S. Shinkai, *Chem. Commun.*, 2009, 2100–2102; (b) A. Dawn, N. Fujita, S. Haraguchi, K. Sada, S. Tamaru and S. Shinkai, *Org. Biomol. Chem.*, 2009, **7**, 4378–4385; (c) B. Escuder, F. Rodríguez-Llansola and J. F. Miravet, *New J. Chem.*, 2010, **34**, 1044–1054; (d) W. Edwards and D. K. Smith, *J. Am. Chem. Soc.*, 2014, **136**, 1116–1124.
- 13 J. Cho, K. Sawaki, S. Hanashima, Y. Yamaguchi, M. Shiro, K. Saigo and Y. Ishida, *Chem. Commun.*, 2014, **50**, 9855–9858.
- 14 (a) V. A. Soloshonok and V. P. Kukhar, *Tetrahedron*, 1996, **52**, 6953–6964; (b) A. Sutherland and C. L. Willis, *J. Org. Chem.*, 1998, **63**, 7764–7769; (c) Y. Ishida, N. Iwahashi, N. Nishizono and K. Saigo, *Tetrahedron Lett.*, 2009, **50**, 1889–1892.
- 15 A. Pal, R. D. Mahapatra and J. Dey, *RSC Adv.*, 2014, **4**, 7760–7765.
- 16 (a) M. C. Etter, *Acc. Chem. Res.*, 1990, **23**, 120–126; (b) C. B. Aakeröy and D. J. Salmon, *CrystEngComm*, 2005, **7**, 439–448.
- 17 (a) P. Sahoo, V. G. Puranik, A. K. Patra, P. U. Sastry and P. Dastidar, *Soft Matter*, 2011, **7**, 3634–3641; (b) P. Yadav and A. Ballabh, *New J. Chem.*, 2015, **39**, 721–730.
- 18 (a) G. M. Sheldrick, *SHELXL-2013, Programs for the Refinement of Crystal Structures*, University of Gottingen, Germany, 2013; (b) G. M. Sheldrick, *Acta Crystallogr., Sect. C: Struct. Chem.*, 2015, **71**, 3–8.